OL | Organic Letters

pubs.acs.org/OrgLett

Letter

Pyridine Wingtip in $[Pd(Py\text{-}tzNHC)_2]^{2+}$ Complex Is a Proton Shuttle in the Catalytic Hydroamination of Alkynes

Miha Virant,[#] Mateja Mihelač,[#] Martin Gazvoda,* Andrej E. Cotman, Anja Frantar, Balazs Pinter,* and Janez Košmrlj*

Cite This: *Org. Lett.* 2020, 22, 2157−2161

Read Online

ACCESS | Metrics & More | Article Recommendations | Supporting Information

ABSTRACT: The cationic palladium(II) complex **1** of pyridyl-mesoionic carbene ligand catalyzes Markovnikov-selective intermolecular hydroamination between anilines and terminal alkynes into the corresponding imines. The reaction proceeds at room temperature, in the absence of additives, with exquisite selectivity and diverse functional group tolerance. The key intrinsic feature of the catalyst is the pyridine wingtip confined to the proximity of the alkynophilic metal active site, which mimics the function of enzyme-like architectures by assisting entropically favored proton transfers.

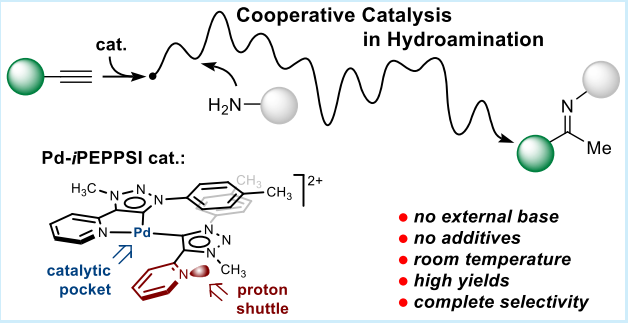

Ligands that provide additional functions beyond their traditional spectator roles are becoming increasingly important in transition-metal catalysis.[1] A metal−ligand cooperation concept has been realized by bifunctional ligands, mostly by establishing control of a catalytic process through weak catalyst−substrate interactions.[2] Examples where the pyridine fragment of such a bifunctional ligand assists the catalytic process by a proton transfer are emerging and have been demonstrated with ruthenium[3a,b] and iridium[3c] catalysts. In palladium catalysis, proton shuttle has been rationalized by an SCS indenediide pincer complex.[3d]

A palladium(II) complex $[Pd(Py\text{-}tzNHC)_2]^{2+}$ $2BF_4^-$ (**1**, Figure 1)[4] was sought ideal for the metal−ligand cooperation

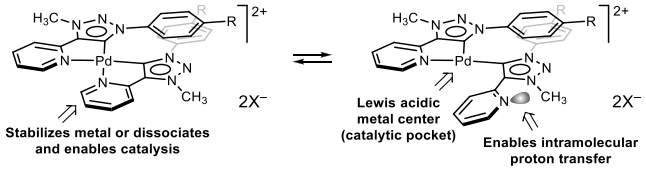

Figure 1. Complexes **1** (R = CH_3) and **1′** (R = H). X = BF_4.

process. While pyridyl-1,2,3-triazol-5-ylidene (Py-*tz*NHC) strongly stabilizes the metal through the mesoionic triazolylidene (*tz*) NHC dent, the more labile pyridine wingtip could play a dual role. By coordination, it internally stabilizes the metal center throughout the preparation of the complex and, more importantly, in the resting state of the catalytic cycle. Upon dissociation, it should expose the Lewis acidic metal center to enable substrates to enter the reactive zone and initiate the catalytic cycle while acting as a local Lewis base functionality in the proximity of the metal, enabling a proton-transfer process.

To test this hypothesis and its potential utility, the intermolecular hydroamination of terminal acetylenes **2** with anilines **3** (Figure 2) was chosen as a model reaction, as it would likely benefit from such a combination of metal/base centers given the multiple proton transfers involved.

Numerous catalysts based on different metals have been developed to promote the intermolecular catalytic hydroamination of terminal acetylenes.[5] Palladium catalysis is rare in hydroamination of terminal alkynes and mostly comprises the examples developed by the groups of Schmidt,[6] Huynh,[7] Cao,[8] and Biffis.[9] These catalysts operate at elevated temperatures (80−100 °C) and require additives (TfOH, AgOTf). The hydroamination is sometimes accompanied by undesired side reactions like cyclotrimerization of alkyne component, consequently requiring a large excess of this reagent.

To assess the utility of **1**, phenylacetylene **2a** and (2,6-dimethyl)aniline **3a** were selected as model substrates. The test reaction was conducted in toluene at room temperature. The selection of this solvent was based on previously documented good performance, albeit the reported transformations took place at substantially higher temperatures (100 °C).[7,8] Monitoring the course of the reaction revealed slow formation

Received: January 14, 2020
Published: January 30, 2020

https://dx.doi.org/10.1021/acs.orglett.0c00203
Org. Lett. 2020, 22, 2157−2161

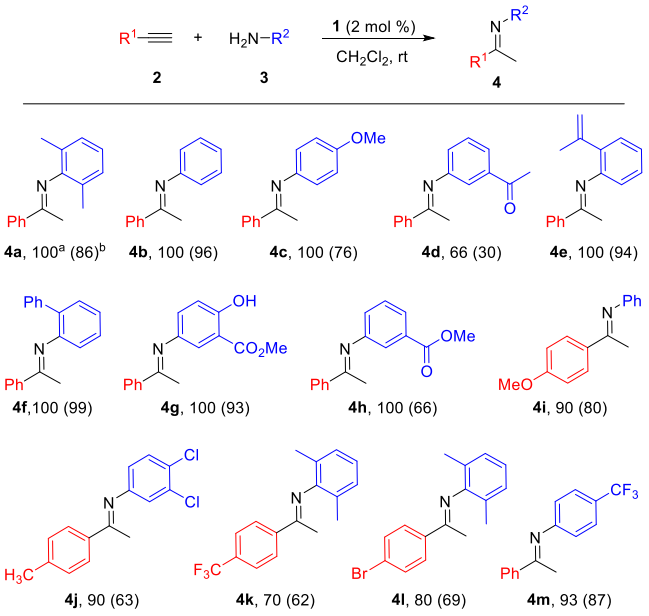

Figure 2. Substrate scope of Pd-catalyzed intermolecular hydroamination. [a] Conversion and [b] isolated percent yields.

of the desired imine **4a**. This promising finding prompted us to screen through the reaction parameters including other solvents, substrates ratios, catalyst loading, and concentrations. This analysis revealed that 1 mol % loading of **1** efficiently promoted hydroamination of phenylacetylene **2a** (1.2 equiv) with (2,6-dimethyl)aniline **3a** (1.0 equiv, 0.5 M) in dichloromethane. Within 24 h at room temperature, the conversion exclusively to the Markovnikov product **4a** was 83%. Besides **4a**, unreacted aniline **3a** (17%) and the excess amounts of acetylene **2a**, without any side product, could be detected as judged by ^{1}H NMR analysis of the crude reaction mixture.

Using these optimal reaction conditions along with somewhat higher catalyst loadings of 2 mol % to ensure higher conversions, we examined the substrate scope of the reaction. As shown in Figure 2, a variety of functional groups is tolerated including hydroxyl (as phenol), methoxy (anisole), methyl, trifluoromethyl, ester, chlorine, bromine, and a C=C double bond in isopropenyl group. Sterically demanding anilines also react well. Excellent results were obtained with acetylene and aniline coupling partners having electron-releasing groups, whereas the presence of electron-deficient substituents slightly eroded the conversions (Figure 2). No isomeric anti-Markovnikov imine could be detected by ^{1}H NMR analyses of the crude reaction mixtures in any of these experiments.

To gauge the direct involvement of the pyridine wingtip into the hydroamination process, we performed the same reaction as described above by using [Pd(ImNHC)] complex **A** and [Pd(Ph-*tz*NHC)] complex **B**. In the latter, the ligand strongly resembles Py-*tz*NHC in **1** with the pyridine wingtip being replaced by phenyl (Figure 3). In contrast to **1**, the pyridine and NHC parts are not bound together in **A** and **B**, allowing the complete dissociation of pyridine from the metal upon engaging in a reaction. No product formation could be observed in the reaction of **2a** and **3a** after 24 h in the presence of these complexes, neither in dichloromethane at room temperature nor in toluene at 100 °C. This striking difference between the activities of **1** and complexes **A** and **B** implies that

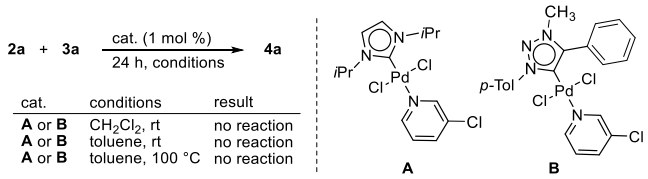

Figure 3. No hydroamination occurs with complex **A** or **B**.

the pyridine wingtip of the *i*PEPPSI ligand indeed plays an explicit role in the overall function of catalyst.

To expose the role of the pyridine wingtip in this catalytic process we scrutinized the mechanism of hydroamination to generate imine product **4b** using solution-state density functional theory (DFT) simulations carried out using DFT as implemented in ORCA 4.0.1.2, employing the method PBE0-D3/def2-SV(P)/RIJCOSX/Grid4,GridX4 for geometry optimizations and PBE0-D3/def2-TZVPP/Grid5,GridX5 for single-point calculations (Supporting Information).[10] Solvation energies in dichloromethane as solvent were computed with the latter computational method, using the SMD implicit solvation model. In our in silico investigation we used slightly truncated model of the complex with 4-tolyl replaced by phenyl group (**1′**, Figure 1). The methyl substituents, relatively far from the metal center and without significant electronic effects, do not affect the general catalytic properties of the [Pd(Py-*tz*NHC)] system and overall energy barriers. Additional details of computational investigations are provided in the Supporting Information. The energy profile of the most likely pathway for the catalytic formation of the imine (**4b**) from phenylacetylene (**2a**) and aniline (**3b**) together with a schematic description of the operative mechanism is illustrated in Figures 4 and 5. In addition, Figure 5 highlights five

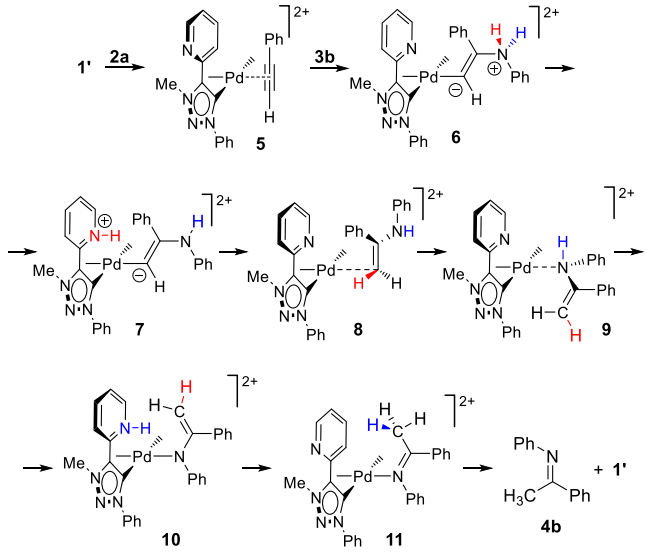

Figure 4. Proposed reaction pathway.

chemically well-identifiable subprocesses, starting with C−N bond formation and terminating with imine dissociation. Competing processes and less likely alternative mechanisms for some of these subprocesses are also discussed in detail in the Supporting Information, together with other pathways that were ruled out due to being unreasonably high in energy.

As expected, and previously proposed for the catalytic hydroamination reactions,[5] the operative pathway begins with

https://dx.doi.org/10.1021/acs.orglett.0c00203
Org. Lett. 2020, 22, 2157−2161

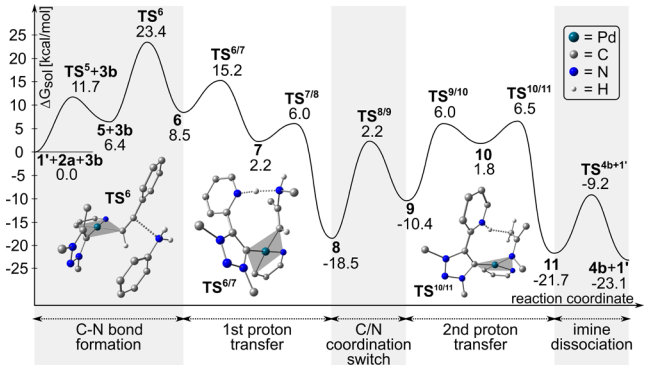

Figure 5. Computational energy trajectory.

acetylene coordination to the catalyst (**1′**) forming the adduct **5** (Figures 4 and 5). In order to accommodate the acetylene substrate in the first coordination sphere of a stable square-planar arrangement, one of the pyridine side arms decoordinates from the Pd(II) center in **5**, allowing tight binding of acetylene to the metal. Although unbound, as being tethered to the mesoionic NHC ring, this pyridine remains in the proximity (<5.0 Å) of the metal forming together a multicenter reactive zone comprising a Lewis base and an acid center. This replacement of the pyridine by the incoming acetylene takes place through an associative interchange process traversing the tbp transition state $\mathbf{TS}^{5}$ with solution-state Gibbs free energy of 11.7 kcal mol^{-1}. The η^2 binding of acetylene to palladium via one of its π bonds activates its carbon atoms toward nucleophilic attack facilitating direct carbon−nitrogen bond formation with the amine substrate. The tell-tale structure of the corresponding transition state ($\mathbf{TS}^{6}$), displayed in Figures 4 and 5, conforms to the expected electronic transitions, namely, binding to the metal through an electron rich carbon meanwhile accepting the lone-pair of the amine at the electron deficient carbon center. This C−N bond formation process is associated with an activation barrier of about 23 kcal mol^{-1}, which is surmountable under standard conditions. While the direct product of this step, complex **6**, is not particularly stable (8.5 kcal mol^{-1}), a subsequent intramolecular proton transfer stabilizes the system.

This proton transfer takes place between the secondary ammonium fragment formed upon C−N bond formation and the liberated pyridine side arm leading to intermediate **7** with an amine substrate and a pyridinium group. A thermodynamically rather stable enamine complex, **8**, is formed upon passing of this pyridinium proton to the carbanion center of the substrate. Both of these proton transfer events are elementary processes associated with a low activation barrier of ∼5−7 kcal mol^{-1} to the preceding intermediates and, accordingly, are facile transformations under the experimental conditions. The structure of $\mathbf{TS}^{6/7}$ (Figures 4 and 5) is evidence that the pyridine side arm has an ideal distance and arrangement to engage in structurally unconfined proton-transfer processes.

To generate the imine product (**4b**) from the enamine substrate in **8**, a formal imine−enamine tautomerism needs to take place along the reaction coordinate. Our simulations imply that such a tautomerism is most effective if the enamine substrate binds to the metal through its amine (N) functionality rather than via its C=C (C) π bond. The requisite C/N coordination switch of the enamine substrate may easily occur in a single step, through $\mathbf{TS}^{8/9}$. The tautomerization process begins from complex **9** with a proton transfer, then again, to the pyridine wingtip forming another transient intermediate with pyridinium functionality (**10**). Traversing $\mathbf{TS}^{10/11}$, shown in Figures 4 and 5, the proton of the pyridinium moiety is transferred to the terminal CH_2 group forming the imine−palladium complex **11**. The two-step process from **9** to **11** is virtually identical to a conventional base-catalyzed imine−enamine tautomerism, but the role of the base is played by the pyridine wingtip of the Py-*tz*NHC ligand.

Finally, the extrusion of the imine product **4b** and the simultaneous regeneration of catalyst **1′** occurs traversing a tbp transition state, $\mathbf{TS}^{4b+1'}$, characterizing a classical associative interchange ligand substitution of the imine to the pyridine side arm. The overall reaction is exergonic by about −23 kcal mol^{-1}.

Evident from the mechanisms of enamine to imine tautomerization and first proton-transfer steps is the explicit role of pyridine in the discovered catalytic reactivity of **1**. Namely, the moderate basicity of pyridine opens low energy reaction channels for the former proton transfer processes through stable pyridinium-containing intermediates, **7** and **10**, with solution-state relative stability of about 2 kcal mol^{-1} to free reactants.

An experimental mechanistic investigation comprising kinetics and KIE studies provides support for the key features of our mechanistic proposal; a method of initial rates for the model reaction between phenylacetylene **2a** and (2,6-dimethyl)aniline **3a** revealed orders of 0.5 in acetylene, 0.3 in aniline, and 1.4 in complex **1**. In addition, the use of deuterated (2,6-dimethyl)aniline ($PhND_2$, **3a**-d_2) leads to a primary KIE of 2.1, whereas the use of PhC≡CD (**2a**-*d*) results in the absence of primary KIE (1.1). These observations are intuitive to interpret by an early pre-equilibrium (**1′** + **2a** = **5**) and a late rate-determining proton-transfer process. Indeed, the imine−enamine tautomerism, i.e., going from **8** to **11**, is associated with an apparent, rate-determining barrier of 25 kcal mol^{-1} centered by $\mathbf{TS}^{10/11}$ and representing proton transfer between the pyridinium group and the terminal CH_2 group, giving rise to the observed primary KIE when using **3a**-d_2. The structure of this rate determining TS accounts for the modest primary kinetic effect when deuterium is transferred—the effect is moderate in comparison to typical KIEs of 5−6 because the structure and bonding of **8** and $\mathbf{TS}^{10/11}$ is significantly different. While the approximate first-order kinetics in the catalyst agrees with a metal-mediated tautomerization process, the dependence of the rate also on the concentrations of acetylene (0.5) and aniline (0.3) is best explained by the slightly uphill pre-equilibrium process between catalyst **1′** and acetylene (**2a**) to form adduct **5** and subsequent C−N bond formation with aniline. Accordingly, these experimental observations are in conceptual agreement with the key features of the mechanism established computationally.

In conclusion, we have demonstrated that beyond mere stabilization and activation of the (pre)catalyst's metal center, the pyridyl-mesoionic carbene ligand in palladium complex $[Pd(Py\text{-}tzNHC)_2]^{2+}$ $2BF_4^-$ efficiently assists the metal along the reaction trajectory in enzyme-like proton transfer events. In transition-metal catalysis, the examples in which the hemilabiltiy of ligands is related to their catalytic properties are still scarce, and to the best of our knowledge, this is the first demonstration of pyridine-assisted proton shuttle in palladium catalysis. We believe this case study is another step toward the

https://dx.doi.org/10.1021/acs.orglett.0c00203
Org. Lett. 2020, 22, 2157−2161

development of novel catalytic systems that are based on these principles.

■ ASSOCIATED CONTENT

Supporting Information

The Supporting Information is available free of charge at https://pubs.acs.org/doi/10.1021/acs.orglett.0c00203.

Experimental procedures and analytical data for the compounds described, computational details, copies of NMR spectra (PDF)

Cartesian coordinates (PDF)

■ AUTHOR INFORMATION

Corresponding Authors

Martin Gazvoda − *Faculty of Chemistry and Chemical Technology, University of Ljubljana, SI-1000 Ljubljana, Slovenia;* orcid.org/0000-0003-3421-0682; Email: martin.gazvoda@fkkt.uni-lj.si

Balazs Pinter − *Departamento de Química, Universidad Técnica Federico Santa María, 2390123 Valparaíso, Chile;* orcid.org/0000-0002-0051-5229; Email: balazs.pinter@usm.cl

Janez Košmrlj − *Faculty of Chemistry and Chemical Technology, University of Ljubljana, SI-1000 Ljubljana, Slovenia;* orcid.org/0000-0002-3533-0419; Email: janez.kosmrlj@fkkt.uni-lj.si

Authors

Miha Virant − *Faculty of Chemistry and Chemical Technology, University of Ljubljana, SI-1000 Ljubljana, Slovenia; Departamento de Química, Universidad Técnica Federico Santa María, 2390123 Valparaíso, Chile;* orcid.org/0000-0002-5919-3631

Mateja Mihelač − *Faculty of Chemistry and Chemical Technology, University of Ljubljana, SI-1000 Ljubljana, Slovenia*

Andrej E. Cotman − *Faculty of Chemistry and Chemical Technology, University of Ljubljana, SI-1000 Ljubljana, Slovenia;* orcid.org/0000-0003-2528-396X

Anja Frantar − *Faculty of Chemistry and Chemical Technology, University of Ljubljana, SI-1000 Ljubljana, Slovenia*

Complete contact information is available at: https://pubs.acs.org/10.1021/acs.orglett.0c00203

Author Contributions

#M.V. and M.M. contributed equally.

Funding

The Slovenian Research Agency (Research Core Funding Grant P1-0230, Project J1-8147, Project J1-9166, and Young Researcher Grant to M.V. including support for his 6-months stay at the Universidad Técnico Federico Santa María), the Ministry of Education, Science and Sport, Republic of Slovenia (PhD Scholarship to M.M.), and the Department of Chemistry of UTFSM are gratefully acknowledged for financial support.

Notes

The authors declare no competing financial interest.

■ ACKNOWLEDGMENTS

CCTVal is acknowledged for the computational resources and Dr. Damijana Urankar from the Research Infrastructure Centre at the Faculty of Chemistry and Chemical Technology University of Ljubljana for HRMS analyses.

■ REFERENCES

(1) (a) Stradiotto, M.; Lundgren, R. J. *Ligand Design in Metal Chemistry: Reactivity and Catalysis*; Wiley, 2016. (b) Kamer, P. C. J.; Leeuwen, P. W. N. M. *Phosphorus(III) Ligands in Homogeneous Catalysis: Design and Synthesis*; Wiley, 2012;. (c) Peris, E.; Crabtree, R. H. Key factors in pincer ligand design. *Chem. Soc. Rev.* **2018**, *47*, 1959−1968.

(2) (a) Crabtree, R. H. Multifunctional ligands in transition metal catalysis. *New J. Chem.* **2011**, *35*, 18−23. (b) Khusnutdinova, J. R.; Milstein, D. Metal−Ligand Cooperation. *Angew. Chem., Int. Ed.* **2015**, *54*, 12236−12273. (c) Peris, E. Smart N-Heterocyclic Carbene Ligands in Catalysis. *Chem. Rev.* **2018**, *118*, 9988−10031. (d) Zhu, J.; Lindsay, V. N. G. Benzimidazolyl Palladium Complexes as Highly Active and General Bifunctional Catalysts in Sustainable Cross-Coupling Reactions. *ACS Catal.* **2019**, *9*, 6993−6998.

(3) (a) Grotjahn, D. B.; Kragulj, E. J.; Zeinalipour-Yazdi, C. D.; Miranda-Soto, V.; Lev, D. A.; Cooksy, A. L. Finding the Proton in a Key Intermediate of anti-Markovnikov Alkyne Hydration by a Bifunctional Catalyst. *J. Am. Chem. Soc.* **2008**, *130*, 10860−10861. (b) Breit, B.; Gellrich, U.; Li, T.; Lynam, J. M.; Milner, Lucy M.; Pridmore, N. E.; Slattery, J. M.; Whitwood, A. C. Mechanistic insight into the ruthenium-catalysed anti-Markovnikov hydration of alkynes using a self-assembled complex: a crucial role for ligand-assisted proton shuttle processes. *Dalton Trans* **2014**, *43*, 11277−11285. (c) Álvarez, E.; Hernández, Y. A.; López-Serrano, J.; Maya, C.; Paneque, M.; Petronilho, A.; Poveda, M. L.; Salazar, V.; Vattier, F.; Carmona, E. Metallacyclic Pyridylidene Structures from Reactions of Terminal Pyridylidenes with Alkenes and Acetylene. *Angew. Chem., Int. Ed.* **2010**, *49*, 3496−3499. (d) Monot, J.; Brunel, P.; Kefalidis, C. E.; Espinosa-Jalapa, N. A.; Maron, L.; Martin-Vaca, B.; Bourissou, D. A case study of proton shuttling in palladium catalysis. *Chem. Sci.* **2016**, *7*, 2179−2187.

(4) For our endeavors in the field, see: (a) Bolje, A.; Košmrlj, J. A Selective Approach to Pyridine Appended 1,2,3-Triazolium Salts. *Org. Lett.* **2013**, *15*, 5084−5087. (b) Gazvoda, M.; Virant, M.; Pevec, A.; Urankar, D.; Bolje, A.; Kočevar, M.; Košmrlj, J. A mesoionic bis(Py-*tz*NHC) palladium(II) complex catalyses ″green″ Sonogashira reaction through an unprecedented mechanism. *Chem. Commun.* **2016**, *52*, 1571−1574. (c) Gazvoda, M.; Virant, M.; Pinter, B.; Košmrlj, J. Mechanism of copper-free Sonogashira reaction operates through palladium-palladium transmetallation. *Nat. Commun.* **2018**, *9*, 4814.

(5) For selected reading, see: (a) Alonso, F.; Beletskaya, I. P.; Yus, M. Transition-Metal-Catalyzed Addition of Heteroatom−Hydrogen Bonds to Alkynes. *Chem. Rev.* **2004**, *104*, 3079−3160. (b) Beller, M.; Seayad, J.; Tillack, A.; Jiao, H. Catalytic Markovnikov and anti-Markovnikov Functionalization of Alkenes and Alkynes: Recent Developments and Trends. *Angew. Chem., Int. Ed.* **2004**, *43*, 3368−3398. (c) Severin, R.; Doye, S. The catalytic hydroamination of alkynes. *Chem. Soc. Rev.* **2007**, *36*, 1407−1420. (d) Wang, Y.; Wang, Z.; Li, Y.; Wu, G.; Cao, Z.; Zhang, L. A general ligand design for gold catalysis allowing ligand-directed anti-nucleophilic attack of alkynes. *Nat. Commun.* **2014**, *5*, 3470. (e) Anokhin, M. V.; Murashkina, A. V.; Averin, A. D.; Beletskaya, I. P. Simple and efficient Au^{I}-based catalyst for hydroamination of alkynes. *Mendeleev Commun.* **2014**, *24*, 332−333. (f) Huang, L.; Arndt, M.; Gooßen, K.; Heydt, H.; Gooßen, L. J. Late transition metal-catalyzed hydroamination and hydroamidation. *Chem. Rev.* **2015**, *115*, 2596−2697.

(6) Shaffer, A. R.; Schmidt, J. A. R. Palladium(II) 3-Iminophosphine Complexes as Intermolecular Hydroamination Catalysts for the Formation of Imines and Enamines. *Organometallics* **2008**, *27*, 1259−1266.

(7) (a) Yuan, D.; Tang, H.; Xiao, L.; Huynh, H. V. CSC-pincer *versus* pseudo-pincer complexes of palladium(II): a comparative study on complexation and catalytic activities of NHC complexes. *Dalton Trans* **2011**, *40*, 8788−8795. (b) Yuan, D.; Huynh, H. V. Sulfur-

functionalized N-heterocyclic carbene complexes of Pd(II): syntheses, structures and catalytic activities. *Molecules* **2012**, *17*, 2491−517. (c) Bernhammer, J. C.; Huynh, H. V. Benzimidazolin-2-ylidene Complexes of Palladium(II) Featuring a Thioether Moiety: Synthesis, Characterization, Molecular Dynamics, and Catalytic Activities. *Organometallics* **2014**, *33*, 1266−1275. (d) Bernhammer, J. C.; Chong, N. X.; Jothibasu, R.; Zhou, B.; Huynh, H. V. Palladium(II) Complexes Bearing an Indazole-Derived *N*-Heterocyclic Carbene and Phosphine Coligands as Catalysts for the Sonogashira Coupling and the Hydroamination of Alkynes. *Organometallics* **2014**, *33*, 3607−3617.

(8) Chen, Q.; Lv, L.; Yu, M.; Shi, Y.; Li, Y.; Pang, G.; Cao, C. Simple, efficient and reusable Pd−NHC catalysts for hydroamination. *RSC Adv.* **2013**, *3*, 18359−18366.

(9) Franco, D.; Marchenko, A.; Koidan, G.; Hurieva, A. N.; Kostyuk, A.; Biffis, A. Palladium(II) Complexes with *N*-Phosphanyl-N-heterocyclic Carbenes as Catalysts for Intermolecular Alkyne Hydroaminations. *ACS Omega* **2018**, *3*, 17888−17894.

(10) Neese, F. The ORCA program system. *WIRE Comput. Mol. Sci.* **2012**, *2*, 73−78.

https://dx.doi.org/10.1021/acs.orglett.0c00203
Org. Lett. 2020, 22, 2157−2161